Part I

Bulk Process Modelling

3D Atomistic Simulations of Submicron Device Fabrication

Marius M. Bunea[†] and Scott T. Dunham[‡]
[†]Department of Physics, [‡]Department of Electrical and Computer Engineering
Boston University, Boston, MA 02215.
http://engc.bu.edu/~mbunea

ABSTRACT

We use the Lattice Monte Carlo method to simulate the coupled motion of vacancies, interstitials and dopants during the annealing of a 50nm channel length NMOS structure. The initial defect locations are taken from Monte Carlo ion implantation simulations. The resulting defects diffuse, recombine, pair and cluster, with rates of these atomic processes calculated based on the local environment. Dopant redistribution occurs via both displacement by vacancies as well as the formation and diffusion of mobile boron and arsenic interstitials. We use these simulations to demonstrate the potential of atomistic simulations for deep submicron devices and to explore the influence of atomistic processes on macroscopic behavior.

INTRODUCTION

It is predicted that by 2012[1] MOS devices will have 50nm channel lengths and 20nm junction depths. A device with these dimensions and a dopant concentration of 10^{19}cm^{-3} has only about 500 dopants in the channel region. At the same time, dopant and defect clusters and/or precipitates, which often control nonequilibrium diffusion processes such as transient enhanced diffusion (TED), are present in much smaller numbers. Therefore, for deep submicron devices the discrete nature of the system and corresponding atomic scale behavior are important. Lattice Monte Carlo[2,3] (LMC) has emerged as an effective method for extending atomistic simulations to times accessible by experiments. There are two reasons for this. On one hand, the fundamental time scale in LMC is the period between hops or transitions (10^{-9}–10^{-6}s) rather than the vibration period (10^{-14}–10^{-13}s) as in molecular dynamics simulations. On the other hand, the method considers only the dopants and defects present in the system which are present in much smaller numbers (10^{10}–10^{21}cm^{-3}) than the atom density ($5 \times 10^{22}\text{cm}^{-3}$). LMC computational requirements scale with device volume (L^3) and are inherently 3D. Thus they become practical as device sizes shrink and 3D effects become more prominent. In contrast, continuum models become more complex and the need for 3D simulations leads to greatly increased simulation times. Thus, there is a convergence when considering deep submicron structures of the need for and the practicality of atomistic simulations.

APPROACH

To provide initial conditions, Monte Carlo ion implant simulations (UT-Marlowe[4]) were performed to generate 3D distributions of dopants, interstitials and vacancies. For the source/drain, arsenic was implanted with an energy of 5 keV and dose of $4\times10^{14}\text{cm}^{-2}$ at

Mat. Res. Soc. Symp. Proc. Vol. 490 © 1998 Materials Research Society

room-temperature into (001) Si with 7° tilt and 30° rotation. The channel doping consisted of a 5keV, 10^{14}cm^{-2} boron implant, again at room-temperature into (001) Si with 7°tilt, 30° rotation. Note that the arsenic implant is masked to appear only in the source/drain region, while the boron channel doping is introduced as a blanket implant over the whole structure. Following the ion implantation, we assumed that in regions where the concentration of interstitials exceeded 5×10^{21}cm^{-3} (10% of atom density) the material was amorphized and later regrew via solid phase epitaxial regrowth into defect-free material (no interstitials or vacancies, all dopants substitutional). Also, since LMC calculations show a very fast initial I/V recombination at the anneal temperature to be simulated (900°C), we take into account nearest neighbor recombination for interstitials and vacancies. The remaining dopants and point defects are then mapped to the nearest sites on the silicon lattice within a box of dimensions 75×75×200 unit cells, which represents a quadrant of an NMOS transistor. The top surface, through which the implant has been made, is assumed to be a perfect sink for defects and all the other surfaces have reflecting boundary conditions based on symmetry considerations.

The LMC method is based on the calculation of the hopping (or transition) rates corresponding to different processes. These rates are assumed to be given by a base rate for a given process (e.g., vacancy migration) in isolation modified by the change in the system energy associated with that hop ($E_i - E_f$):

$$\nu = \nu^0 \exp\left(\frac{-E_m}{kT}\right) \exp\left(\frac{E_i - E_f}{2kT}\right), \tag{1}$$

where ν^0 includes the vibration frequency and entropy of migration, E_m is the migration energy, k is the Boltzmann constant and T is the absolute temperature. Thus the hopping rate is increased if the system energy after the hop (E_f) is smaller than before the hop (E_i) and reduced if the system energy is increased.

In the course of the simulation, hopping rates are calculated for all mobile species in the system, taking into account only hops to first nearest neighbor sites. At each step, a hop is chosen randomly, weighted by the relative rates. The time is then incremented by an amount given by the inverse sum of the rates:

$$\Delta t = \left[\sum_{i=1}^{N}\sum_{j=1}^{4} \nu_{ij}\right]^{-1}, \tag{2}$$

where N is the number of mobile species in the system and the second sum accounts for the four possible hop directions. Transition rates are recalculated in the neighborhood of the hop which just occurred and a new hop is chosen, advancing the system in time.

The mobile species considered in this work are vacancies, interstitials, and dopant interstitials. The interactions considered are: dopant/vacancy binding leading to both vacancy-mediated diffusion as well as the formation of arsenic/vacancy clusters; dopant/interstitial binding leading to the formation of immobile dopant/interstitial pairs and clusters (particularly boron/interstitial clusters or BICs); dopant kick-out via interstitials leading to the formation of mobile interstitial dopants; interstitial/interstitial binding leading to the formation of interstitial clusters (e.g., {311} defects); and vacancy/vacancy binding leading to the formation of vacancy clusters. Migration and binding energies used in the simulations are presented in Table I and are based where possible on experimental results and *ab-initio*

Table I: Parameters used in lattice Monte-Carlo simulations.

binding energies	migration energies	exchange, kick-in and kick out barriers
E(As-V)=1.18 eV[6]	E_m^{V}=0.3 eV[8]	E_{exch}(As-V)=0.66 eV[6]
E(As$_s$-I)=0.6 eV	E_m^{I}=0.9 eV[5]	E_{exch}(B-V)=2.5 eV[7]
E(As$_i$-As$_s$)=0.0 eV	$E_m^{\mathrm{B}_i}$=0.3 eV[5]	$E_{\mathrm{kick-out}}$(B)=1.0 eV[5]
E(B-V)=0.17 eV[7]	$E_m^{\mathrm{As}_i}$=0.3 eV	$E_{\mathrm{kick-in}}$(B)=0.6 eV[5]
E(B$_s$-I)=1.0 eV[5]		
E(B$_i$-B$_s$)=1.8 eV[5]		
E(I-I)=0.6 eV		
E(V-V)=0.3 eV		

calculations (references cited in table). For this work, only first nearest neighbor interactions were considered. For interstitial arsenic, *ab-initio* results are not available, so we assume arsenic/interstitial interaction similar to boron but with smaller binding energy for the As$_s$-I pair and no binding for the As$_i$-As$_s$ pair.

RESULTS

In Figure 1 we present a 3D illustration of the locations of dopants in one quadrant of the NMOS structure immediately after the ion implantation ($t = 0$), and after simulation by LMC of annealing at 900°C for 10ms and 0.1s. In Figure 2, we show the total number of point

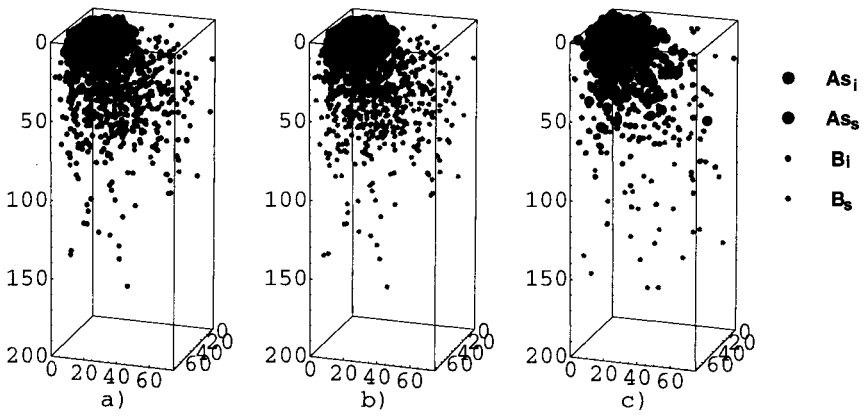

Figure 1: A quadrant (75×75×200 unit cells) of a 50nm NMOS transistor where we show the dopants, arsenic and boron, in substitutional or interstitial state, (a) after ion implant simulation ($t = 0$). Also shown is the evolution of this system during an anneal at 900°C after (b) 10^4ns (10μs) and (c) 10^8ns (0.1s).

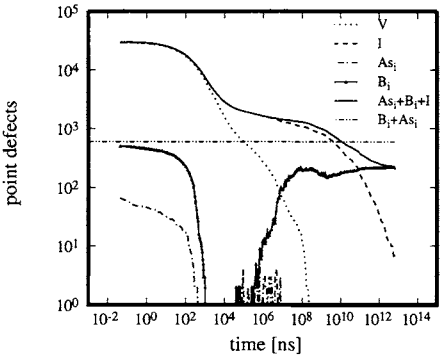

Figure 2: The number of vacancies, interstitials, dopant interstitials as functions of time. The horizontal line represents the total number of dopant interstitials at the beginning of LMC simulation.

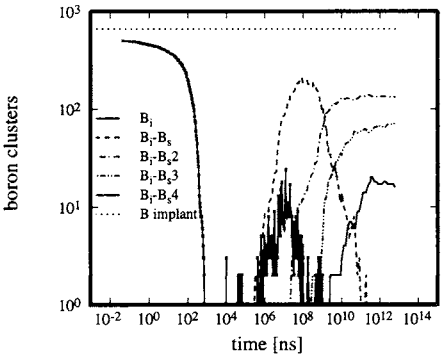

Figure 3: The number of boron interstitial clusters as function of time. Horizontal line is the number of boron atoms implanted.

defects and interstitial dopants as functions of time. The time evolution of boron clusters is shown in Figure 3. Initially, vacancies and interstitials are present in large and nearly equal numbers. The boron atoms are primarily interstitial, but a large fraction of arsenic atoms are substitutional due to the epitaxial regrowth. As the vacancy diffusivity (and thus hopping rate) is substantially larger than that of interstitials,[5,8] the dominant processes initially are vacancy/silicon exchanges and I/V recombination. On the same time scale, dopants go from the interstitial to the substitutional state, primarily due to interactions with vacancies.

In the time interval between 10^3 and 10^5ns (1 to 100μs), almost the entire boron dose is substitutional (Fig. 3). This behavior can be explained by noting that as long as the numbers of interstitials and vacancies are comparable, the much larger hopping frequency of vacancies will cause vacancy capture by dopants to dominate over interstitial capture. The numbers of interstitial dopants and dopant/interstitial clusters only starts to increase when almost all of the free vacancies are gone. After 10^6ns (1ms) vacancies exist almost solely in the form of arsenic/vacancy clusters. This is illustrated further by Figure 4, which shows the evolution of point defects for a boron implant identical with the one used for initializing the MOS device. Here we see that the disappearance of vacancies coincides with the appearance of boron/interstitial complexes (pairs and clusters).

Between 10^5 and 10^8ns (10μs and 0.1s), the concentration of interstitials is relatively stable as most of the interstitials are tied up in interstitial clusters. Note that this concentration is slightly larger than the total implant dose (boron plus arsenic) outside the amorphized region as some of the vacancies find the surface before recombining with interstitials, resulting in a greater than 1+ remaining interstitial dose. Also during this time period, the concentration of boron interstitials is increasing. The number of boron/interstitial pairs reaches a maximum at 10^8ns (0.1s) when we also see a peak in the total number of boron interstitials in Fig. 2. These boron interstitials migrate through the lattice, leading to the formation of successively larger clusters (Fig. 3). After about 10^{10}ns (10s) the {311} defects dissolve,

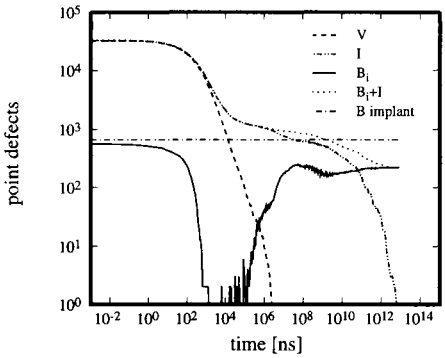

Figure 4: Number of vacancies, interstitials and boron interstitials as functions of time for the annealing of a boron implant, 5keV, 10^{14}cm^{-2}, 7° tilt, 30° rotation. Horizontal line is the number of boron ions implanted.

causing a drop in the total number interstitials as they diffuse to the top surface sink. Due to the cluster energetics,[5] although larger clusters form, the dominant species remains B_3I (B_i-B_s2 in Fig. 3). We find the behavior of boron clusters to be very much dependent on the binding energy between interstitial and substitutional boron. For the energetics used in these simulations, these clusters are quite stable and do not dissociate over the simulation times used (up to 10^{13}ns or about 3 h).

CONCLUSIONS

We have developed a 3D atomistic simulator that takes into account the range of processes occurring during ion implant annealing: vacancy/dopant and vacancy/silicon exchanges, I/V recombination, dopant/defect and defect/defect interactions, interstitial and dopant interstitial migration, and clustering and emission from clusters. The simulations provide insight into the atomic scale details of dopant and point defect interactions during ion implant annealing. We have shown through a demonstration on a 50nm channel length MOS transistor structure that such simulations can be used for deep submicron devices. We expect further work on faster algorithms as well as advancement in computational hardware will reduce the required run times (about 50h on an SGI Origin2000 workstation in this work) to that appropriate for everyday use of LMC simulations. The atomic scale interaction energies are critical to the behavior of the system and further investigation both experimentally as well as via *ab-initio* calculations will be necessary for the production of a predictive atomistic simulator.

ACKNOWLEDGMENTS

The authors would like to thank Jing Zhu, Oleg Pankratov, Jeff Nelson and Tomas Diaz de la Rubia for information on the results of their *ab-initio* calculations as well as valuable discussions. Funding for this work was provided by the Semiconductor Research Corporation. Computer resources were provided through the Boston University Center for Computational Science.

REFERENCES

[1]The National Technology Roadmap for Semiconductors (Semiconductor Industry Association, 1997).

[2]S. T. Dunham and C. D. Wu, *J. Appl. Phys.* **78**, 2362 (1995).

[3]M. M. Bunea and S. T. Dunham, in **Defects and Diffusion in Silicon Processing**, ed. by S. Coffa, T. D. de la Rubia, C. S. Rafferty, and P. Stolk (Mat. Res. Soc. Proc. 469, Pittsburgh, PA, 1997).

[4]S. Tian, S. J. Morris, B. Obradovic, M. F. Morris, G. Wang, G. Balamurugan, A. F. Tasch, and C. Snell, **UT-Marlowe User Manual**, (Univ. of Texas at Austin, 1997).

[5]J. Zhu, T. Diaz de la Rubia, L. H. Yang, C. Mailhiot and G. H. Gilmer, *Phys. Rev B* **54**, 4741 (1996).

[6]O. Pankratov, H. Huang, T. D. de la Rubia, in **Microstructure Evolution During Irradiation**, ed. by I. M. Robertson, G. S. Was, L. W. Hobbs, T. D. de la Rubia, (Mat. Res. Soc. Proc. 439, Pittsburgh, PA, 1996).

[7]J. S. Nelson (private communication).

[8]G. D. Watkins, J. R. Troxell and A. P. Chatterjee, in **Defects and Radiation Effects in Semiconductors**, ed. by J. H. Albany (Inst. Phys. Conf. Ser. No. 46, 1979) p. 16.

ARSENIC DEACTIVATION IN SILICON

M.A. BERDING, A. SHER

Applied Physical Sciences Laboratory, SRI International, 333 Ravenswood Ave., Menlo Park, CA 94025, marcy@plato.sri.com

ABSTRACT

In this paper we examine the properties of arsenic in silicon, using *ab initio* calculations and a statistical theory. Good agreement is found between theory and experiment for the electronic concentration as a function of temperature and total arsenic concentration. We show that for low arsenic concentrations, full activation is the equilibrium condition. In equilibrium, the neutral complex composed of a lattice vacancy surrounded by four arsenic ($V\mathrm{As}_4$) is the dominant means by which high concentrations of arsenic are rendered inactive. Under constrained equilibrium conditions in which $V\mathrm{As}_4$ cluster formation is prohibited, we show that $V\mathrm{As}_3\mathrm{Si}_1$ cluster populations increase dramatically and can account for nearly the same degree of compensation as the $V\mathrm{As}_4$ clusters. Even $V\mathrm{As}_2$ clusters alone can account for substantial deactivation in the absence of $V\mathrm{As}_3$ and $V\mathrm{As}_4$ clusters. These smaller complexes are essential not only to the establishment of equilibrium, since SiAs_4 clusters are extremely rare, but can also explain some degree of deactivation, even if the formation of $V\mathrm{As}_4$ clusters are kinetically inhibited.

INTRODUCTION

Understanding the process and kinetics of arsenic deactivation in silicon is of great interest for both technological and scientific reasons; this includes an understanding of deactivated arsenic structures and how those structures form. Many models have been proposed [1-3]. with good fits to selected sets of experimental data. Experimental evidence now suggests that vacancies are present during deactivation [4-9]. Theoretically, Pandey et al. have shown the $V\mathrm{As}_4$ cluster as an energetically favorable structure [4]. However, entropy disfavors the formation of such a large defect complex, and a complete free energy calculation is therefore needed to determine the role of $V\mathrm{As}_4$ in deactivation. Because arsenic ions repel one another in the absence of a vacancy, there are also fundamental questions as to the pathway and time constant for the formation of such a large defect complex, since the number of SiAs_4 clusters is quite low. Ramamoorthy and Pantelides [10] examined other defect clusters involving arsenic in the context of arsenic diffusion, but do not consider the ionized states or the entropy which, as we show, are important and lead to conclusions in disagreement with theirs. Finally, no one-cluster deactivation model can explain the reverse annealing phenomenon [11,12]. To explain this phenomenon and have a physically based model requires either a multiple-cluster model or precipitation [12,13].

In this paper we examine the behavior of arsenic in silicon using a statistical mechanical model. *No fitting to deactivation data was done*, and the only experimental data used in the calculations relate to the temperature-dependent band structure, which were deduced from totally separate experiments. The energies for various defect complexes were taken from *ab initio* calculations. Unlike previous calculations, we consider the full free energy to determine the deactivation mechanism, including the temperature-dependent electronic excitations and the entropy.

Mat. Res. Soc. Symp. Proc. Vol. 490 © 1998 Materials Research Society

APPROACH

The statistical mechanical model is based on a generalized quasichemical approximation formalism [14] which has been extended to include the chemical potential of the electronic subsystem using full Fermi-Dirac statistics [15]. In the method, the real space zinc blende lattice (including both lattice and interstitial sites) that the atoms and defects occupy is divided into clusters, each containing n lattice sites. Here we use non-overlapping clusters with $n = 5$, corresponding to one lattice site surrounded by its four nearest neighbors on the diamond lattice. Each distinguishable class of cluster j is assigned an energy E_j which is assumed to depend only on the average environment. It can be shown [15] that the average fractional population $y_{j,q}$ of the j^{th} distinguishable cluster type with charge q can be written as a function of the neutral cluster energies E_j, defect ionization energies $\epsilon_{j,q}$, cluster degeneracies $g_{j,q}$, the constituent chemical potentials μ_i, the Fermi energy μ_f, and the temperature and pressure. The cluster energies and ionization energies are calculated (see following paragraph) and degeneracies deduced. Thus the set of cluster populations $y_{j,q}$ for a system containing two chemical constituents, silicon and arsenic, are functions of five unknowns: μ_{Si}, μ_{As}, μ_F, T, and P. The system was treated as a single phase system, with the arsenic concentration fixed to what is present following a laser melt anneal [16]. From Gibbs's phase rule there are three degrees of freedom for a single phase system containing two components, which we set by choosing T, P, and the arsenic concentration [As]. Two additional equations needed to determine the unknowns are the normalization condition on the cluster populations $\sum_{j,q} y_{j,q} = 1$, and the condition of overall charge neutrality.

Electronic contributions to the cluster free energies E_j were obtained from a full-potential version of the linearized muffin-tin orbital method [17], in the local density functional approximation (LDA) with the Barth and Hedin functional [18]. Five-atom cluster energies were extracted from 32-atom supercell total energies, where each supercell contains the 5-atom cluster surrounded by bulk silicon, and full relaxation of the lattice was allowed. To ensure a good fit to the charge density and potential in the interstitial region, empty spheres have been included, and orbitals added to the basis by centering them on the empty spheres. The semi-core d electrons on the arsenic atoms were treated explicitly as valence states in a second panel. The basis set and charge density representation was chosen so as to give errors in the cluster energies less than 0.01 eV. For the highest symmetry cells, relaxation calculations were performed using two special k-points, and final energies were calculated using fourteen special k-points. More k-points were used for lower symmetry cells. The core was allowed to relax during the self-consistency cycle.

Various defects for deactivation were examined: lattice vacancies surrounded by from zero to four arsenic; silicon and arsenic interstitials; and clusters involving multiple arsenic atoms both on lattice sites and interstitially, with and without lattice vacancies involved. Only defects containing lattice vacancies are found to be important in explaining the deactivation, and therefore in this letter we restrict our discussion to the six most important clusters: the bulk silicon cluster Si_5; substitutional arsenic surrounded by four silicon atoms As_1Si_4; and a lattice vacancy surrounded by from one to four arsenic atoms as near neighbors: $V\mathrm{As}_1\mathrm{Si}_3$, $V\mathrm{As}_2\mathrm{Si}_2$, $V\mathrm{As}_3\mathrm{Si}_1$, and $V\mathrm{As}_4$. Experimental values for the electron and hole density of states effective mass [19] and experimental values of the temperature-dependent band gap by extrapolating from the low temperature expression given in ref. [19], are used. At elevated temperatures, the acceptor and donor levels deduced from the zero-temperature LDA calculations are assumed to track the valence and conduction bands, respectively.

RESULTS

Equilibrium Properties

Energies of various five-atom clusters are given in Table I; clusters with very high energies and correspondingly negligible densitities are not included. Ionization energies for each of the clusters are also summarized in Table I. The $V\mathrm{As}_4$ cluster is found to be neutral and strongly bound with respect to isolated arsenic and bulk silicon, in agreement with Pandey et al. [4]. The $V\mathrm{As}_3\mathrm{Si}_1$ and $V\mathrm{As}_2\mathrm{Si}_2$ clusters are found to have one and two acceptor levels,